BIOCHEMISTRY
including biophysical chemistry & molecular biology
Article

Biochemistry **2009,** *48,* 11075–11083 11075
DOI: 10.1021/bi9012462

The SH2 Domains of Inositol Polyphosphate 5-Phosphatases SHIP1 and SHIP2 Have Similar Ligand Specificity but Different Binding Kinetics[†]

Yanyan Zhang, Anne-Sophie Wavreille, Andrew R. Kunys, and Dehua Pei*

Department of Chemistry and Ohio State Biochemistry Program, The Ohio State University, 100 West 18th Avenue, Columbus, Ohio 43210

Received July 21, 2009; Revised Manuscript Received October 17, 2009

ABSTRACT: SH2 domain-containing inositol 5-phosphatases 1 (SHIP1) and 2 (SHIP2) are structurally similar proteins that catalyze the degradation of lipid secondary messenger phosphatidylinositol 3,4,5-triphosphate to produce phosphatidylinositol 3,4-diphosphate. Despite their high sequence identity (51%), SHIP1 and SHIP2 share little overlap in their *in vivo* functions. In this work, the sequence specificity of the SHIP2 SH2 domain was systematically defined through the screening of a combinatorial pY peptide library. Comparison of its specificity profile with that of the SHIP1 SH2 domain showed that the two SH2 domains have similar specificities, both recognizing pY peptides of the consensus sequence pY[S/Y][L/Y/M][L/M/I/V], although there are also subtle differences such as the tolerance of an arginine at the pY + 1 position by the SHIP2 but not SHIP1 SH2 domain. Surface plasmon resonance analysis of their interaction with various pY peptides suggested that the two domains have similar binding affinities but dramatically different binding kinetics, with the SHIP1 SH2 domain having fast association and dissociation rates while the SHIP2 domain showing apparent slow-binding behavior. Site-directed mutagenesis and kinetic studies indicated that the SHIP2 SH2 domain exists as a mixture of two conformational isomers. The major, inactive isomer apparently contains two *cis* peptidyl−prolyl bonds at positions 88 and 105, whereas the minor, active isomer has both proline residues in their *trans* configuration. *Cis*−*trans* isomerization of the peptidyl−prolyl bonds may provide a potential mechanism for regulating the interaction between SHIP2 and pY proteins. These data suggest that a combination of tissue distribution, specificity, and kinetic differences is likely responsible for their *in vivo* functional differences.

Phosphoinositides are components of the cell membrane and act as important signaling molecules that regulate cell proliferation and survival, cytoskeletal reorganization, and vesicular trafficking by recruiting effector proteins to cellular membranes (*1*). For example, activated cell-surface receptors recruit and activate phosphoinositide 3-kinases (PI3K),[1] which phosphorylate phosphatidylinositol 4,5-diphosphate [PtdIns(4,5)P_2] to produce phosphatidylinositol 3,4,5-triphosphate [PtdIns(3,4,5)P_3]. PtdIns(3,4,5)P_3 in turn recruits pleckstrin homology (PH) domain-containing proteins such as the serine/threonine kinase Akt to the plasma membrane for further downstream signaling events (*2*). To regulate the cellular levels of lipid secondary messengers such as PtdIns(3,4,5)P_3, cells utilize two major types of phosphoinositide phosphatases. The inositol polyphosphate 3-phosphatase PTEN hydrolyzes the 3-phosphate group of PtdIns(3,4,5)P_3 to form PtdIns(4,5)P_2 (*3*). PtdIns(3,4,5)P_3 is also degraded at the 5-phosphate position by a family of inositol polyphosphate 5-phosphatases (5-ptases) to form PtdIns(3,4)P_2, which can undergo further hydrolysis to form PtdIns3P (*4*). Among the 10 mammalian 5-ptases, two contain a Src homology 2 (SH2) domain, SH2 domain-containing inositol 5-phosphatases 1 (SHIP1) and 2 (SHIP2). SHIP1 is a 145 kDa protein containing an N-terminal SH2 domain, a central catalytic 5-ptase domain, two NPXY motifs capable of interacting with phosphotyrosine-binding (PTB) domains, and a C-terminal proline-rich region. SHIP2 (142 kDa) contains an N-terminal SH2 domain, a catalytic domain, a single NPXY site, and a C-terminal sterile α motif (SAM) domain. Despite their high sequence homology (51% identity) and similar domain architecture, SHIP1 and SHIP2 have little overlap in their *in vivo* functions (*4*). SHIP1 plays a major role in mediating the inhibitory signaling in B cells and mast cells and is a negative regulator of cell growth (*5*−*7*). SHIP2 acts as an inhibitor of the insulin signaling pathway (*8*−*10*). One reason for their distinct functions is undoubtedly their different expression patterns: SHIP1 is predominantly expressed in hematopoietic cells, whereas SHIP2 is more ubiquitously expressed, most prominently in skeletal muscle, heart, and brain (*11*−*14*). However, even in cells that express both SHIP1 and SHIP2 (e.g., platelets and macrophages), the two enzymes play nonredundant roles (*15*, *16*). Thus, the noncatalytic structural elements in SHIP1 and SHIP2 must play a role in dictating their *in vivo* functions, likely through

[†]This work was supported by a grant from the National Institutes of Health (GM062820).

*To whom correspondence should be addressed. Telephone: (614) 688-4068. Fax: (614) 292-1532. E-mail: pei.3@osu.edu.

[1]Abbreviations: Abu or U, 2-L-aminobutyric acid; BCIP, 5-bromo-4-chloro-3-indolyl phosphate; IPTG, isopropyl β-D-thiogalactoside; ITAM, immunoreceptor tyrosine-based activation motif; ITIM, immunoreceptor tyrosine-based inhibition motif; MBP, maltose-binding protein; PED-MS, partial Edman degradation−mass spectrometry; PH domain, pleckstrin homology domain; PI3K, phosphoinositide 3-kinases; PTB, phosphotyrosine binding; PtdIns(4,5)P_2, phosphatidylinositol 4,5-diphosphate; PtdIns(3,4,5)P_3, phosphatidylinositol 3,4,5-triphosphate; pY, phosphotyrosyl; SA-AP, streptavidin−alkaline phosphatase; RU, response unit; SAM, sterile alpha motif; SH2 domain, Src homology 2 domain; SHIP1, SH2 domain-containing inositol 5-phosphatase 1; SPR, surface plasmon resonance.

Published on Web 10/19/2009

binding to different partner proteins. The SH2 domains of SHIP1 and SHIP2, which share 54% sequence identity, may recognize different phosphotyrosyl (pY) proteins. Previous studies have shown that the SH2 domain of SHIP1 binds tyrosine-phosphorylated Shc (*17*), the Gabs (Grb2-associated binders) (*18*, *19*), the Doks (downstream of tyrosine kinases) (*20*−*22*), protein tyrosine phosphatase SHP-2 (*23*, *24*), c-Cbl (*25*), and LAT (linker for activation of T-cells) (*26*). The SHIP2 SH2 domain has been shown to bind to $p130^{Cas}$ (*27*). In addition, both SHIP1 and SHIP2 can bind via their SH2 domains to the immunoreceptor tyrosine-based activation motifs (ITAMs) and immunoreceptor tyrosine-based inhibition motifs (ITIMs) of cell-surface receptors such as those of FcγRIIB and FcεRI (*28*−*33*). These observations suggest that the SH2 domains of SHIP1 and SHIP2 may have overlapping and yet distinct binding specificities. The detailed specificity profile of the SHIP1 SH2 domain has previously been defined by screening a pY peptide library (*34*), but similar data for the SHIP2 SH2 domain are not yet available. In this work, we subjected the SHIP2 SH2 domain to the same library screening procedure and determined its detailed specificity profile. A comparison of the two domains reveals that they have similar but not identical binding specificities. Interestingly, our studies show that the two domains bind to their pY targets with dramatically different kinetic behaviors, which likely contribute to their different *in vivo* functions.

MATERIALS AND METHODS

Materials. The pMAL-c2 vector, all DNA modifying enzymes, and amylose resin were purchased from New England Biolabs (Ipswich, MA). The pET-28a vector was purchased from Novagen (Gibbstown, NJ). All oligonucleotides were purchased from Integrated DNA Technologies (Coralville, IA). 5-Bromo-4-chloro-3-indolyl phosphate (BCIP), antibiotics, *N*-hydroxysuccinimido-biotin, Sephadex G-25 resin, 4-hydroxy-α-cyanocinnamic acid, and organic solvents were obtained from Sigma-Aldrich (St. Louis, MO). Talon resin for IMAC purification was purchased from Clontech (Mountain View, CA). Reagents for peptide synthesis were from Advanced ChemTech (Louisville, KY), Peptides International (Louisville, KY), and NovaBiochem (La Jolla, CA). The SHIP1 SH2 domain was prepared as previously described (*34*). Protein concentration was determined by OD_{280} and the Bradford method using bovine serum albumin as standard.

Expression, Purification, and Biotinylation of SHIP2 SH2 Domain. The DNA coding for SHIP2 SH2 domain (amino acids 1−121) was subcloned from pcDNA3-SHIP2 (kindly provided by Dr. S. Tridandapani of The Ohio State University) by the polymerase chain reaction (PCR) with the following primers: 5′-GGAATTCATGGCCTCAGTGTGTGGGACA-3′ and 5′-CCCAAGCCTTTATCTCTCCCCCTCTACA-3′. The PCR product was digested with restriction endonucleases *Eco*RI and *Hin*dIII and ligated into the corresponding sites in pMAL-c2 or pET-28a vectors. The resulting constructs expressed SHIP2 SH2 domain as fusion proteins containing an N-terminal maltose-binding protein (MBP) or a six-histidine tag. SHIP2 SH2 domain mutants were generated in the pET construct using the QuikChange mutagenesis kit (Stratagene) and the following primers: P88S, 5′-GACCTCACAGGGTGTTTCTGTGCGTCGCTTCCAGAC-3′ and 5′-GTCTGGAAGCGACGCACAGAAACACCCTGTGAGGTC-3′; P105E, 5′-GGCCTATATGCCCAGGAGAACCAGGGTCTTGTTTGTGCC-3′ and 5′-GGCACAAACAAGACCCTGGTTCTCCTGGGCATATAGGCC-3′. The authenticity of each DNA construct was confirmed by DNA sequencing of the entire coding region.

For protein expression, *Escherichia coli* DH5α cells harboring plasmid pMAL-c2-SHIP2 SH2 or BL21(DE3) cells harboring plasmid pET28a-SHIP2 SH2 were grown at 37 °C in LB medium to OD_{600} ∼0.6. The cells were induced by the addition of 0.1 mM isopropyl β-D-thiogalactoside (IPTG) and allowed to grow for 4 h at 30 °C. The cells were harvested by centrifugation and lysed in a French pressure cell in the presence of protease inhibitors. MBP-SH2 and His-tagged SH2 domains were purified by amylose and Talon cobalt affinity columns, respectively, following the manufacturer's instructions. The histidine-tagged SH2 protein was further passed through a Sephadex G-25 column to exchange the Talon column elution buffer into a buffer suitable for surface plasmon resonance (SPR) analysis (10 mM Hepes, 150 mM NaCl, 3 mM EDTA, pH 7.4). The MBP-SH2 protein (5 mg) was concentrated to ∼4 mg/mL and treated with 2.5 equiv of *N*-hydroxysuccinimido-biotin for 30 min at 4 °C, followed by the addition of 10 μL of 1 M Tris, pH 8.0. After 10 min of incubation, the biotinylated MBP-SH2 protein was passed through a Sephadex G-25 column to remove any excess biotin, flash frozen in the presence of 33% (v/v) glycerol, and stored at −80 °C.

Library Screening. The pY peptide library was synthesized as previously described (*34*). Typically, 30−50 mg of the pY-containing library was placed in a micro Bio-Spin column (0.8 mL; Bio-Rad), washed exhaustively with DCM and DMF, and incubated in a blocking buffer (30 mM HEPES, pH 7.4, 150 mM NaCl, 0.1% gelatin, and 0.05% Tween 20) for 1 h. The resin was drained and resuspended in 800 μL of fresh blocking buffer containing 20 nM biotinylated MBP-SH2 protein. After overnight incubation at 4 °C with gentle mixing, the resin was drained and resuspended in 800 μL of SA-AP buffer (30 mM Tris, pH 7.4, 250 mM NaCl, 10 mM $MgCl_2$, 70 μM $ZnCl_2$, and 20 mM K_2HPO_4) containing 1 μg of streptavidin−alkaline phosphatase (SA-AP). The mixture was incubated for 10 min at 4 °C. The resin was then drained and quickly washed twice with 300 μL of SA-AP high salt buffer (30 mM Tris, pH 7.4, 500 mM NaCl, 10 mM $MgCl_2$, 70 μM $ZnCl_2$), twice with 300 μL of the blocking buffer, and twice with 300 μL of SA-AP reaction buffer (30 mM Tris, pH 8.5, 100 mM NaCl, 5 mM $MgCl_2$, 20 μM $ZnCl_2$). The resin was transferred to a Petri dish with 900 μL of the SA-AP reaction buffer, and 100 μL of a fresh BCIP solution (5 mg/mL in SA-AP reaction buffer) was added. Turquoise color developed on positive beads at ∼30 min, when the staining reaction was quenched with the addition of ∼1 mL of 2 M HCl for 5 min. The resin was transferred back into the Bio-Spin column and washed extensively with a 0.1% Tween 20 solution to remove any unreacted BCIP substrate. Positive beads were manually removed from the library with a micropipet under a dissecting microscope and individually sequenced by partial Edman degradation−mass spectrometry (PED-MS) as previously described (*35*, *36*). Control experiments with biotinylated MBP produced no colored beads under identical conditions.

Synthesis of Biotinylated pY Peptides. Each peptide was synthesized on 50 mg of Clear-amide resin (0.46 mmol/g) using standard Fmoc/HBTU/HOBt chemistry. D-Biotin was coupled to the N-terminus of each peptide via a miniPEG-Asn-Asn linker or to the side chain of a C-terminal lysine. Ninhydrin test was used to monitor the completion after each coupling reaction. After cleavage and deprotection with a modified reagent K (6.5% phenol, 5% water, 5% thioanisole, 2.5% ethanedithiol,

1% anisole in TFA), the crude peptides were purified by reversed-phase HPLC on a C_{18} column (Varian 120 Å, 4.6 × 250 mm). The identity of the peptides was confirmed by MALDI-TOF mass spectrometric analyses.

SPR Analysis. All measurements were made at room temperature on a BIAcore 3000 instrument. Biotinylated pY peptides were immobilized onto a streptavidin-coated sensorchip. A sensorchip with reduced pY peptide loading was generated by passing a 1:10 (mol/mol) mixture of biotinylated pYSYL peptide (10 nM) and free biotin (100 nM) over a streptavidin-coated chip to give an increase of 10 response units (RU). Comparison of RU_{max} values at saturating protein concentrations indicated that the actual pY peptide loading was reduced by ~20-fold. Increasing concentrations of an N-terminal histidine-tagged SH2 protein (0−6.4 μM) in HBS-EP buffer (10 mM HEPES, pH 7.4, 150 mM NaCl, 3 mM EDTA, and 0.005% polysorbate 20) were passed over the sensorchip for 120−600 s at a flow rate of 15−30 μL/min. A blank flow cell (no immobilized pY peptide) was used as control to correct for any signal due to the solvent bulk and/or nonspecific binding interactions. In between two runs, the sensorchip surface was regenerated by flowing a strip solution (10 mM NaCl, 2 mM NaOH, and 0.025% SDS in H_2O) for 5−10 s at a flow rate of 100 μL/min. The RU_{eq} at a given SH2 protein concentration was obtained by subtracting the response of the blank flow cell from that of the sample flow cell. The dissociation constant (K_D) was obtained by nonlinear regression fitting of the data to the equation, $RU_{eq} = RU_{max}[SH2]/(K_D + [SH2])$, where RU_{eq} is the measured response unit at a certain SH2 protein concentration and RU_{max} is the maximum response unit. Kinetic data were obtained by globally fitting the sensorgrams (after subtraction of background from blank flow cell) to predefined models using BIAevaluation software (version 4.1) according to the manufacturer's instructions. The models employed in this work were based on "1:1 binding with mass transfer" to include different bulk refractive index changes at the beginning and end of injections. Mass transport constant (k_t) and χ^2 values were constantly monitored to ensure the quality of the fitting.

RESULTS

Sequence Specificity of SHIP2 SH2 Domain. We screened the SHIP2 SH2 domain against a one-bead-one-compound (OBOC) pY peptide library previously employed for the SHIP1 SH2 domain, H_2N-TAXXpYXXXLNBBRM-resin [where B is β-alanine and X represents any of the 18 proteinogenic amino acids except for Cys and Met plus 2-L-aminobutyric acid (Abu or U) and norleucine (Nle or M) as Cys and Met surrogates] (*34*). The N-terminal dipeptide (TA) reduces any potential bias caused by the free N-terminus (which is required for peptide sequencing). The linker sequence (LNBBRM) was included to facilitate peptide release (CNBr cleavage after Met) and MALDI MS analysis (Arg provides a fixed positive charge, whereas Leu-Asn shifts the peptide mass to >600 Da to avoid overlapping with matrix signals). The two β-alanine residues provide a flexible linker to facilitate the binding of a target protein to the immobilized peptides. The theoretical diversity of the library is 20^5 or 3.2×10^6. The library was synthesized on TentaGel microbeads (90 μm) and screened against the biotinylated MBP-SHIP2 SH2 domain. Beads containing high-affinity ligands for the SH2 domain recruited the biotinylated MBP-SH2 protein to their surface, which in turn recruited the streptavidin−alkaline phosphatase (SA-AP) conjugate to the beads. Upon the addition of BCIP, the alkaline phosphatase hydrolyzed BCIP to generate a turquoise precipitate deposited on the bead surface.

Table 1: pY Sequences Selected against SHIP2 SH2 Domain (85 Total)[a]

VRpYALU	XXpYDLU	UYpYRYU	YApYSMU	UQpYYYA
XDpYALU	XMpYDPM	WUpYRHI	AKpYSMU	XXpYYKU
IQpYALU[b]	NApYFLU	XXpYRMI	RQpYSMU	FDpYYLU
RSpYALU	XXpYFLV	UWpYRYI	AGpYSVU	NGpYYLU
RIpYAYU	UUpYKLU	XXpYRVL	VApYSYU[b]	YGpYYLU
RNpYAYU	XQpYKLU	YSpYRYL	VApYSYU	SGpYYRU
GRpYAYU	AApYLFU	STpYRYL	AUpYSYU	TTpYYYU
UPpYAYU	AGpYLIU	AYpYRTM	UHpYSYU	XXpYYYU
TPpYAYU	XEpYPYU	EEpYRTV	ANpYSYU	
VKpYUFU	UVpYRYA	FGpYSYA	VQpYSYU	WYpYVRH
GDpYUFU	IApYRFU	FApYSFU	LVpYSYU	RGpYWFQ
UApYULU	XLpYRLU	AMpYSFU	DGpYSYI	XXpYYTR
VApYULU	SMpYRLU	XQpYSFU	GGpYSYI	XXpYMTR
XXpYULU	ULpYRLU	RYpYSFU	XVpYSYL	XXpYRWY
YRpYUYU	VTpYRLU	IApYSLU	SMpYTYU	
SUpYUFU	XWpYRMU	XGpYSLU	XXpYTLV	
AApYUFL	XFpYRYU	QRpYSLU	XXpYVLU	
GGpYULV	FTpYRYU[b]	GApYSMU	XXpYXLU	

[a]Sequences were obtained from two screening experiments performed at 20 nM SHIP2 SH2 domain. [b]Peptides selected for further binding analysis: U, α-L-aminobutyric acid; M, norleucine; X, amino acids whose identity could not be unambiguously determined.

A total of 100 mg of the pY peptide library (~3×10^5 beads) was screened against the SHIP2 SH2 domain, and 93 intensely colored beads were isolated from the library and sequenced by the PED-MS method (*35*, *36*) to give 85 binding sequences (Table 1). Inspection of the selected sequences reveals that the SHIP2 SH2 domain has very broad specificity on the N-terminal side of pY but is highly selective on the C-terminal side (Figure 1). At the pY+3 position, Abu (which was used as a Cys surrogate), is most preferred, although other aliphatic hydrophobic amino acids including Leu, Ile, and Val were also selected. SHIP2 SH2 domain also strongly prefers a hydrophobic residue at the pY+2 position, with Tyr being most frequently selected, followed by Leu, Phe, and Nle. Interestingly, the SH2 domain recognizes two completely different classes of residues at the pY+1 position: the first class possesses small residues Ser, Ala, and Abu, whereas the second class includes Arg and Tyr, both of which contain amphipathic side chains. A few peptides that do not fall into the above consensus sequences (pYVRH, pYWFQ, pYMTR, pYYTR, and pYRWY) are likely false positives caused by nonspecific interactions and not further pursued.

Comparison of the Sequence Specificities of SHIP1 and SHIP2 SH2 Domains. A comparison of the above data with the sequences previously selected against the SHIP1 SH2 domain (*34*) reveals that the two SH2 domains have overlapping but not identical sequence specificities (Figure 1). On the N-terminal side of pY, both SH2 domains have broad specificities, though there are some subtle differences. The SHIP1 domain selected a proline at position pY−2 among 18% of all sequences, but the SHIP2 domain did not select proline at all at the same position. On the other hand, the SHIP2 domain selected a significant number of arginines at position pY−2 (11%) while SHIP1 did not. The two domains also prefer the same set of amino acids at the pY+2 position (Leu, Tyr, Nle, and Phe), although the ranking order of these four amino acids are different. For the SHIP1 SH2 domain, the most frequently selected residue was leucine, while Tyr was the most dominant residue for SHIP2 SH2 domain. The main difference between the two domains is at the pY+1 position, where SHIP1 SH2 domain showed a strong

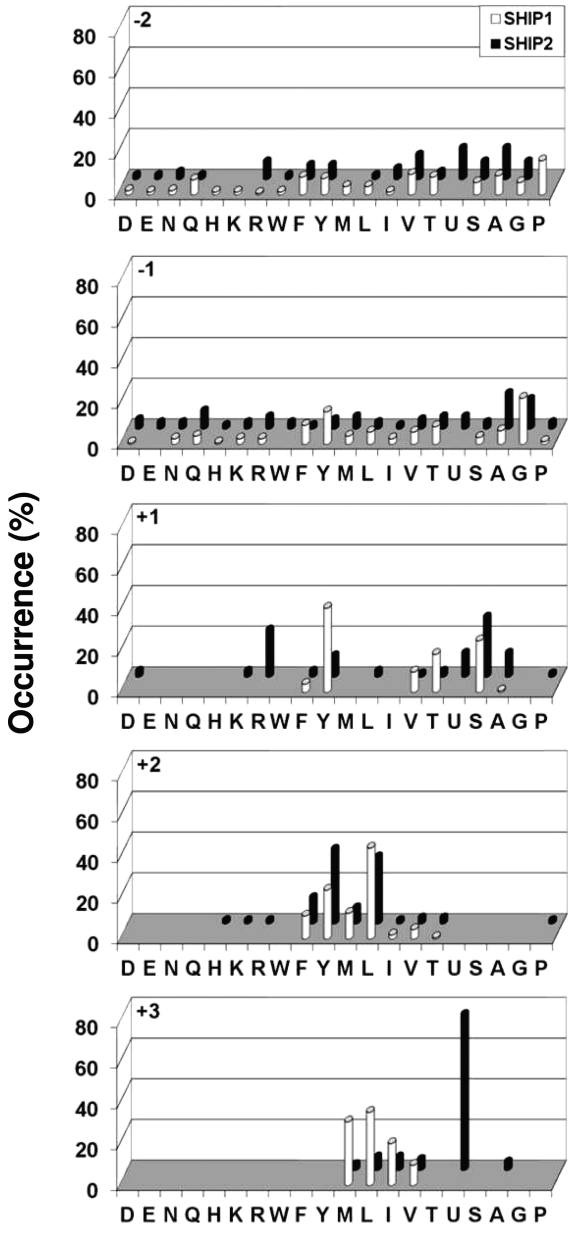

FIGURE 1: Sequence specificities of SHIP1 and SHIP2 SH2 domains. The histograms represent the amino acids identified at each position from pY−2 to pY+3. Percentile of occurrence on the *y* axis represents the percentage of selected sequences that contain a particular amino acid at a certain position. Key: open bar, SHIP1 SH2 domain; closed bar, SHIP2 SH2 domain; M, norleucine; U, 2-L-aminobutyrate.

preference for Tyr, followed by Ser, Thr, and Val. The most preferred residues for the SHIP2 SH2 domain are small amino acids Ser, Ala, and Abu. Tyr is also selected, but at a much lower frequency as compared to SHIP1 domain (11% vs 42%). The most striking difference, however, is the recognition of Arg at the pY+1 position by the SHIP2 domain, which was completely absent among the SHIP1-binding sequences. At the pY+3 position, both SH2 domains require a hydrophobic, aliphatic residue. The SHIP2 SH2 has a strong preference for Abu. Since our previous screening of the SHIP1 SH2 domain was carried out with a pY library that did not contain Abu at the random region, we rescreened the new library against the SHIP1 SH2 domain and found that the SHIP1 domain strongly prefers Leu and Nle over Abu, Val, and Ile (data not shown).

Binding Affinities of Selected Peptides. To confirm the library screening results, three representative sequences, VApYSYC, IQpYALC, and FTpYRYC (Table 2, peptides 1, 4, and 5), were individually synthesized and tested for binding to SHIP1/2 SH2 domains by SPR analysis. To determine the effectiveness of Abu as the Cys surrogate, we also synthesized peptides 2 and 3, which are identical to peptide 1 except that the Cys at the pY+3 position is replaced with Leu and Abu, respectively (Table 2). Peptide 5 was chosen because it contains an Arg at the pY+1 position, which was not selected by the SHIP1 SH2 domain. Peptide 6 (PFpYSLL) is a high-affinity ligand of the SHIP1 SH2 domain, identified from our previous library screening (*34*). Peptides 7−9 correspond to the ITIM/ITAM motifs in immunoglobulin G receptor proteins FcγRIIB (ITpYSLL) and FcγRIIA (GGpYMTL and NIpYLTLG), which are known to bind to SHIP1/2 SH2 domains *in vivo* (*37*). They are employed here as the benchmarks for comparison. Peptide 3 (VApYSYU), which was the actual sequence selected from the peptide library, bound to the SHIP2 SH2 domain with high affinity (K_D = 0.64 μM) and slightly less tightly to the SHIP1 SH2 domain (K_D = 0.89 μM). Substitution of Leu for the Abu residue had little effect on the binding affinities. In contrast, substitution of Cys for Abu reduced the affinities to both SH2 domains by 7.5-fold (Table 2, compare peptides 1 and 3). These results indicate that the SHIP1/2 SH2 domains do not prefer but may be able to tolerate a Cys at the pY+3 position. Peptides 1, 4, and 5 had similar K_D values to the SHIP2 SH2 domain (4.8, 2.9, and 5.2 μM, respectively), indicating that Ser, Ala, and Arg are similarly preferred at the pY+1 position, as the screening data have suggested (Figure 1). On the other hand, peptide 5 (pYRYC) has ~3-fold lower affinity than peptide 1 (pYSYC) toward the SHIP1 SH2 domain (K_D values of 17 and 6.6 μM), again in agreement with our previous library screening data (i.e., the SHIP1 SH2 domain does not prefer an Arg at the pY+1 position) (*34*). Peptide 6 (pYSLL), an optimal ligand selected against the SHIP1 SH2 domain (*34*), binds to the SHIP1 SH2 domain 14-fold more tightly than the SHIP2 domain (K_D values of 0.23 and 3.2 μM, respectively). In comparison, peptide 2 (pYSYL) bound the SHIP2 SH2 domain 5-fold better than peptide 6, again in agreement with the screening results (i.e., SHIP1 prefers a Leu whereas SHIP2 prefers a Tyr at the pY+2 position). Peptide 7, which also contains the pYSLL motif, binds to SHIP1 with ~4-fold

Table 2: Dissociation Constants (K_D, μM) of SHIP1 and SHIP2 SH2 Domains against pY Peptides

peptide	peptide sequence[a]	SHIP1[b]	SHIP2[b]
1	VApYSYC	6.6 ± 0.5	4.8 ± 0.6
2	VApYSYL	0.87 ± 0.09	0.61 ± 0.05
3	VApYSYU	0.89 ± 0.09	0.64 ± 0.09
4	IQpYALC	2.3 ± 0.2	2.9 ± 0.3
5	FTpYRYC	17 ± 4	5.2 ± 0.7
6	PFpYSLL	0.23 ± 0.03	3.2 ± 0.4
7	ITpYSLL	0.40 ± 0.05	1.5 ± 0.2
8	GGpYMTL	0.84 ± 0.07	1.0 ± 0.1
9	NIpYLTLG	1.6 ± 0.1	2.9 ± 0.9

[a]Peptides 1−5 each contained biotin-miniPEG-NN at the N-terminus and LNR-NH_2 at the C-terminus. Peptide 6 was acetylated at the N-terminus and contained a C-terminal linker, LNBK(PEG-biotin)R-NH_2 (B, β-alanine). Peptides 7−9 were biotinylated at their N-termini and contained the following sequences: peptide 7, biotin-EAENTITpYSLLKH; peptide 8, biotin-ETA-DGGpYMTLNPRAPTDDDKNIYLTLG; peptide 9, biotin-ETADGGY-MTLNPRAPTDDDKNIpYLTLG. [b]SPR conditions: SHIP1 SH2 domain was flowed over the surface for 120 s at 15 μL/min, while SHIP2 SH2 domain was flowed for 600 s at 20 μL/min.

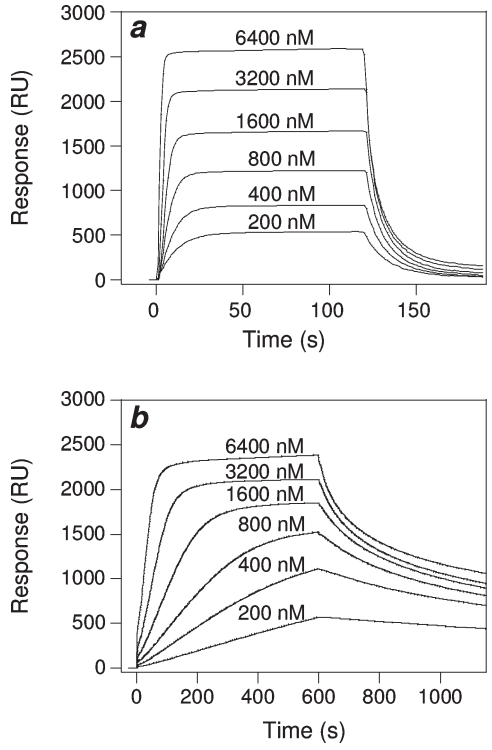

FIGURE 2: SPR sensorgrams for the binding of SHIP1 (a) and SHIP2 SH2 domains (b) to immobilized peptide 2 (VApYSYL). Varying concentrations of the SH2 domains (200−6400 nM) were flowed over the sensorchip for 120 s (SHIP1) or 600 s (SHIP2).

higher affinity than SHIP2. Comparison of peptides 6 and 7 suggests that residues on the N-terminal side of pY or beyond the pY+3 position may also have some (though relatively minor) influence on the overall binding affinity (*34*, *38*, *39*). Finally, the two ITAM motifs bound to SHIP1/2 domains with similar affinities (Table 2). In summary, the quantitative binding studies are in excellent agreement with the library screening results.

Differential Binding Kinetics of SHIP1 and SHIP2 SH2 Domains. During our initial SPR studies, we noticed that the SHIP1 and SHIP2 SH2 domains exhibited drastically different binding kinetics. The SHIP1 SH2 domain bound to the immobilized ligands with fast "on" and "off" rates, and the binding equilibrium was reached very quickly (< 30 s) even at low protein concentrations (Figure 2a). In contrast, the SHIP2 domain showed both very slow association and dissociation rates; at lower protein concentrations (e.g., 200−400 nM), the binding equilibrium was not reached even after passing the protein solution for 10 min at a higher flow rate (20 μL/min, as compared to 15 μL/min for SHIP1) (Figure 2b). This slow-binding behavior made it difficult to accurately determine the equilibrium dissociation constants (K_D) because failure to reach binding equilibrium at low protein concentrations underestimates their equilibrium response units (RU_{eq}), which in turn results in artificially high apparent K_D values (or an underestimate of the binding affinity). We therefore attempted to determine the association (k_{on}) and dissociation rates (k_{off}) of the binding interactions and calculate the dissociation constants (k_D) from the corresponding kinetic constants ($k_D = k_{off}/k_{on}$). Six pY peptides (peptides 2, 3, 6, and 7−9) were selected for the detailed kinetic investigation by SPR, and their k_{on} and k_{off} values were obtained by global fitting of SPR sensorgrams obtained at several different SH2 domain concentrations (200−6400 nM) against a predefined binding model. We initially explored a simple binding model for a bimolecular interaction as described in eq 1 (model I).

Table 3: Kinetic Properties of SHIP1 SH2 Domain[a]

peptide	k_t ($\times 10^{-5}$ m s^{-1})	k_{on} ($\times 10^5$ M^{-1} s^{-1})	k_{off} (s^{-1})	k_D (μM)	K_D (μM)	$t_{1/2}$ (s)
2	1.6	10.9	0.85	0.78	0.87 ± 0.09	0.82
3	1.4	3.1	0.29	0.95	0.89 ± 0.09	2.4
6	3.0	3.0	0.048	0.16	0.23 ± 0.03	14
7	2.0	10.5	0.29	0.28	0.40 ± 0.05	2.4
8	1.0	2.9	0.23	0.79	0.84 ± 0.07	3.1
9	1.1	5.9	0.80	1.4	1.6 ± 0.1	0.87

[a] k_t is the diffusion rate constant. K_D is the equilibrium dissociation constant derived from nonlinear regression fitting of the data to the equation $RU_{eq} = RU_{max}[SH2]/(K_D + [SH2])$. k_D is the dissociation constant calculated from the association and dissociation rate constants ($k_D = k_{off}/k_{on}$). $t_{1/2}$ (half-life of the protein−peptide complex) is derived from $t_{1/2} = \ln 2/k_{off}$.

$$\begin{aligned} P_{bulk} &\underset{k_{-t}}{\overset{k_t}{\rightleftharpoons}} P_{sensor} \\ P_{sensor} + L &\underset{k_{off}}{\overset{k_{on}}{\rightleftharpoons}} PL \end{aligned} \quad (1)$$

In this model, P is the SH2 domain and L is the immobilized pY peptide. This model includes a transport step for diffusion of the SH2 domain from the bulk solution to the sensor surface, to correct for any effect of mass transport limitation (*40*). At high association rates and/or high binding capacity, diffusion of the protein from the bulk to the sensor surface becomes rate-limiting. As shown in Table 3, the interaction between the SHIP1 SH2 domain and the six pY peptides is well described by this model, and the k_D values derived from the kinetic studies are very similar to the respective K_D values obtained from equilibrium binding experiments. The rates of association (k_{on}) are typically on the order of 10^5 M^{-1} s^{-1}, while the dissociation rates (k_{off}) are 0.23−0.85 s^{-1}, corresponding to half-lives ($t_{1/2}$) of 0.82−3.1 s for the SH2 domain−pY peptide complexes (except for peptide 6, which for yet unknown reasons gave poor fitting in all experiments). The fitting produced mass transport rates (k_t) in the range of (1−2) $\times$ 10^{-5} m s^{-1}, in excellent agreement with the k_t values reported for other SH2 domains (*40*). Global fitting of the SHIP2 data to the above model gave k_{on} and k_{off} values that are 2 orders of magnitude lower than the corresponding values of the SHIP1 SH2 domain, consistent with a slow-binding mechanism (Table 4). However, the k_t values obtained were in the range of 0.021−0.042 $\times$ 10^{-5} m s^{-1}, which are ~40-fold lower than that of SHIP1 or other SH2 domains. Since the rate of diffusion of a protein is independent of its binding properties, this large deviation in the k_t value indicates that the above model is inadequate to describe the binding behavior of the SHIP2 SH2 domain.

Effect of P88S and P105E Mutations on SHIP2 SH2 Domain Binding Properties. We theorized that a time-dependent conformational change in the SHIP2 SH2 domain structure may be responsible for the observed "slow-binding" behavior. A possible mechanism may involve the *cis*−*trans* isomerization of a peptidyl−prolyl bond. It has previously been reported that isomerization of a peptidyl−prolyl bond in the SH2 domain of interleukin-2 tyrosine kinase (Itk) alters its binding affinity to pY peptides (*41*), although its effect on the binding kinetics has not yet been investigated. Sequence alignment of the SHIP1/2 SH2 domains revealed the SHIP2 domain contains two extra prolyl

Table 4: Kinetic Properties of SHIP2 SH2 Domain[a]

		model I					model II				
peptide	K_D (μM)	k_t ($\times 10^{-5}$ m s^{-1})	k_{on} ($\times 10^5$ M^{-1} s^{-1})	k_{off} (s^{-1})	k_D (μM)	$t_{1/2}$ (s)	k_t ($\times 10^{-5}$ m s^{-1})	k_{on} ($\times 10^5$ M^{-1} s^{-1})	k_{off} (s^{-1})	k_D (μM)	$t_{1/2}$ (s)
2	0.61 ± 0.05	0.042	0.14	0.0026	0.18	270	1.7	5.7	0.0026	0.0046	270
3	0.64 ± 0.09	0.042	0.090	0.0011	0.12	630	1.7	3.6	0.0011	0.0029	630
6	3.2 ± 0.4	617	0.007	0.0012	1.8	580	440	1.4	0.0051	0.037	140
7	1.5 ± 0.2	0.032	0.060	0.0017	0.29	410	1.2	2.4	0.0017	0.0072	410
8	1.0 ± 0.1	0.028	0.067	0.0022	0.33	320	1.1	2.7	0.0022	0.0083	320
9	2.9 ± 0.9	0.021	0.22	0.0041	0.18	170	0.84	9.0	0.0041	0.0045	170

[a] k_t is the diffusion rate constant. K_D is the equilibrium dissociation constant derived from nonlinear regression fitting of the data to the equation $RU_{eq} = RU_{max}[SH2]/(K_D + [SH2])$. k_D is the dissociation constant calculated from the association and dissociation rate constants ($k_D = k_{off}/k_{on}$). $t_{1/2}$ (half-life of the protein−peptide complex) is derived from $t_{1/2} = \ln 2/k_{off}$.

```
SHIP1  WNHGNITRSKAEELLSRTGKDGSFLVRASESISRAYALCVLYRNCVYTYRILPNEDDKFT 64
SHIP2  WYHRDLSRAAAEELLARAGRDGSFLVRDSESVAGAFALCVLYQKHVHTYRILPDGEDFLA 80

SHIP1  VQASEGVSMRFFTKLDQLIEFYKKENMGLVTHLQYPV 101
SHIP2  VQTSQGVPVRRFQTLGELIGLYAQPNQGLVCALLLPV 117
```

FIGURE 3: Sequence alignment of human SHIP1 and SHIP2 SH2 domains using ClustalW2 (*47*). The two extra proline residues in SHIP2 are shaded in gray.

residues at positions 88 and 105 that are absent in the SHIP1 SH2 domain (Figure 3). We mutated the two prolyl residues to the corresponding amino acids in SHIP1 (Ser and Glu, respectively) and assessed the binding properties of the mutant SH2 domains against peptides 2 and 7 by SPR. To our gratification, both P88S and P105E mutants exhibit faster association kinetics than the wild-type protein, while the dissociation rates are relatively unchanged (Figure 4a−c). Curve fitting against model I gave apparent k_{on} values of 14000, 88000, and 21500 M^{-1} s^{-1} and k_{off} values of 0.0026, 0.0020, and 0.0028 s^{-1} for WT, P88S, and P105E proteins, respectively (Table 5). Thus, the P88S and P105E mutants bind to peptide 2 with 7.8- and 1.4-fold higher affinities than the WT SHIP2 protein. The apparent K_D values derived from equilibrium binding studies also suggested that the P88S mutant has ~3-fold higher affinity than the WT protein. Similar tends were observed with peptide 7 (data not shown).

Reanalysis of SHIP2 SH2 Domain Kinetics Using Improved Binding Model. While the simple binding model described above was inadequate for the SHIP2 domain, we found that all of the experimental results can be rationalized by a modified model as described in eq 2 (model II).

$$\begin{gathered} P \underset{}{\overset{K}{\rightleftharpoons}} P^* \\ P^*_{bulk} \underset{k_{-t}}{\overset{k_t}{\rightleftharpoons}} P^*_{sensor} \\ P^*_{sensor} + L \underset{k_{off}}{\overset{k_{on}}{\rightleftharpoons}} P^*L \end{gathered} \qquad (2)$$

In model II, P represents the SHIP2 SH2 domain with Pro-88 and Pro-105 in the *cis* configuration, whereas P* is the active form of protein with the prolines in the *trans* configuration. We assume that P is incapable of binding or binds only weakly to the pY ligands. K is the equilibrium constant between Pand P* in the absence of pY ligands, k_{on} is the association rate constant for P* and pY ligand, and k_{off} is the dissociation rate constant of the P*L complex. We also assume that interconversion between P and P* is slow and negligible under the SPR conditions. This assumption is reasonable since *cis*−*trans* isomerization of a peptidyl−prolyl bond involves an activation barrier of ~20 kcal/mol (*42*) and the interconversion between P and P* requires the isomerization of two such bonds. Our data suggest that the SHIP2 SH2 domain exists predominantly in its inactive form (P) with only a minor component in the active form (P*). During SPR analysis, because the concentration of P* is low, the association phase is at least partially limited by mass transport. The apparent k_{on} value derived from curve fitting (against model I) in Table 4 is likely a function of both the intrinsic k_{on} value of P*−pY interaction and the rate of P* delivery to the surface. After an extended mass transport period (which corresponds to the initial linear region of the sensorgrams), a sufficient amount of P* is bound to the immobilized ligands, and an equilibrium is reached between free P* and P*L (as indicated by the plateau region of the sensorgram). This model is consistent with our observation that higher flow rates (30 vs 15 μL/min) increase the apparent association rate and shorten the mass transport phase during SPR analysis (data not shown).

To estimate the K value for WT SHIP2 SH2 domain, we compared the apparent association rates of WT and P88S proteins, as reflected by the slopes of the initial linear region of the sensorgrams (Figure 4a,b). The apparent association rates of the P88S protein were consistently ~40-fold higher than those of the WT protein under the same experimental conditions. If one assumes that the two proteins (in their P* forms) have the same intrinsic k_{on} value (which is not unreasonable since they have similar k_{off} values suggesting that Pro-88 is not directly involved in ligand binding), the different rates suggest that the P88S mutant has ~40-fold more protein in the P* form than the WT SH2 domain. If one further assumes that the P88S protein is all in the P* form (which is clearly an overestimate), it would suggest that ~2.5% of the WT SHIP2 SH2 domain exists in the P* form (or $K \sim 0.025$). We next performed curve fitting of the SHIP2 SH2 sensorgrams against model II with a K value of 0.025, and the results are summarized in Table 4. The quality of the fitting is reflected by the k_t values obtained, which are in the range of $1.4-2.8 \times 10^{-5}$ m s^{-1} and similar to those of SHIP1 and other SH2 domains (*40*). Fitting against the modified model gave the same dissociation rates ($k_{off} = 0.0011-0.0041$ s^{-1}) and half-lives for the P*L complexes (170−630 s) as did with model I (except for peptide 6). On the other hand, the new model gave much higher

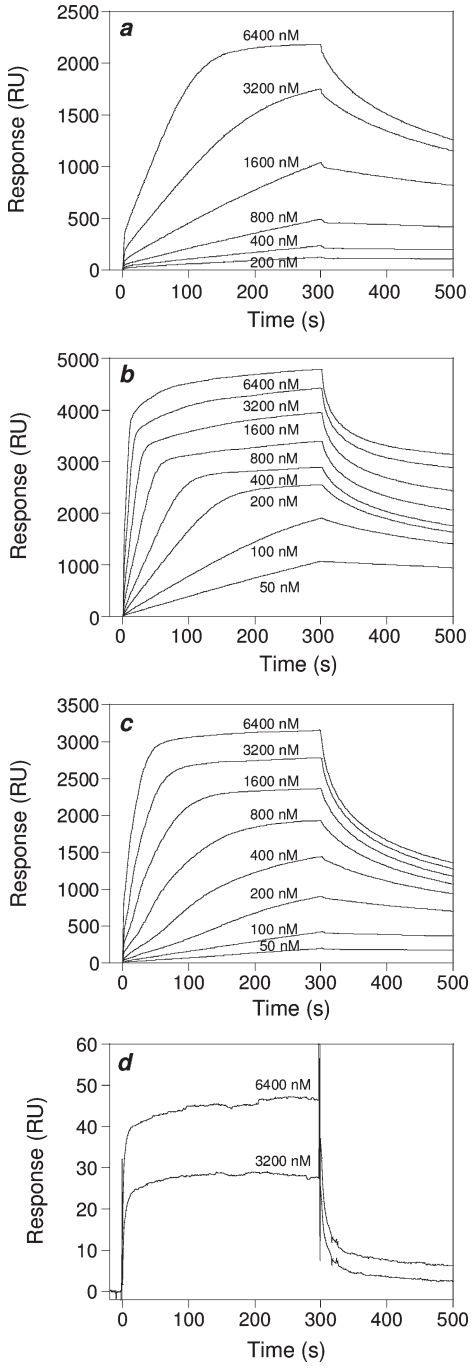

FIGURE 4: SPR sensorgrams for the binding of WT and mutant SHIP2 SH2 domains to immobilized peptide 2 (VApYSYL): (a) WT SH2 domain; (b) P88S mutant; (c) P105E mutant; (d) WT SH2 domain. Sensorgrams in (a)−(c) were obtained on a chip loaded with a normal amount of pY peptide, whereas the sensorgram in (d) was from a chip containing 20-fold reduced pY peptide loading. Varying concentrations of proteins (50−6400 nM) were flowed over the surface at 30 μL/min.

k_{on} values (2.4−9.0 × 10^5 M^{-1} s^{-1}), which are similar to those of the SHIP1 SH2 domain (Table 3). Thus, the active form of SHIP2 SH2 domain (P*) is an exceptionally tight binder of pY ligands, with k_D values of 2.9−8.2 nM for peptides 2, 3, 7, 8, and 9. The apparent slow-binding behavior observed by SPR was caused by mass transport limitation (*40*). The higher apparent K_D values derived from equilibrium binding analysis were caused by overestimation of the active protein concentration (by ~40-fold) and failure to reach equilibrium at lower protein concentrations and should be corrected according to the equation

Table 5: Binding of WT and Mutant SHIP2 SH2 Domains to Peptide 2 (pYSYL)[a]

protein	k_t ($\times 10^{-5}$ m s^{-1})	k_{on} ($\times 10^5$ M^{-1} s^{-1})	k_{off} (s^{-1})	k_D (μM)	K_D (μM)
WT (model I)	0.042	0.14	0.0026	0.18	0.61 ± 0.05
WT (model II)	1.7	5.7	0.0026	0.0046	0.61 ± 0.05
P88S	0.90	0.88	0.0020	0.023	0.19 ± 0.02
P105E	0.22	0.22	0.0028	0.13	0.59 ± 0.04

[a] k_t is the diffusion rate constant. K_D is the equilibrium dissociation constant derived from nonlinear regression fitting of the data to the equation $RU_{eq} = RU_{max}[SH2]/(K_D + [SH2])$. k_D is the dissociation constant calculated from the association and dissociation rate constants ($k_D = k_{off}/k_{on}$). Data for P88S and P105E mutants were derived from fitting against model I because their K values were not available.

$k_D = K_D^{app}/K$. This model provides a simple explanation for the higher apparent binding affinities of the P88S and P105E mutants relative to the WT protein, because the Ser and Glu residues in the mutants should exist in the *trans* configuration, increasing the population of the P* form proteins (larger K value).

Finally, to provide additional support for model II, we generated a sensorchip with 20-fold reduced pY ligand loading and used it examine the binding kinetics of the WT SHIP2 SH2 domain. We anticipated a shorter mass transport phase on this sensorchip (as compared to those in Figures 2 and 4a), because less protein is needed to reach binding equilibrium. This is indeed the case; in fact, the slow mass transport phase essentially disappeared (Figure 4d). Unfortunately, the poor signal/noise ratio caused by the low ligand loading made it difficult to perform any quantitative analysis.

DISCUSSION

In order to gain insight into the molecular basis for the functional difference between SHIP1 and SHIP2, we employed a combinatorial peptide library approach to systematically define the sequence specificity of the SHIP2 SH2 domain and compared it with that of the SHIP1 SH2 domain. Our results show that the two SH2 domains have overlapping (though nonidentical) specificities, both capable of binding to pY peptides of the consensus sequence pY[S/Y][L/Y/M][L/M/I/V] (Figure 1). This is consistent with the previous reports that SHIP1 and SHIP2 bound to the same ITAM, ITIM, and ITAM-like motifs on cell-surface receptors, which have the general consensus of pYXX(L/I) (*28*−*33*, *43*). Their requirement for a hydrophobic residue at the pY+2 position (e.g., Leu and Tyr) makes SHIP1/2 SH2 domains rather unique among the SH2 domain family, as most of them have little selectivity or prefer hydrophilic residues at this position. Our study also revealed some notable differences between the SHIP1/2 SH2 domains. For example, the SHIP2 SH2 domain accepts Arg at the pY+1 position, whereas the SHIP1 SH2 domain does not (Figure 1 and Table 2). At the pY+2 position, the SHIP1 domain prefers Leu over Tyr, while the SHIP2 domain has the opposite preference (Figure 1 and Table 2). At the pY+3 position, SHIP1 has a slight preference for the larger hydrophobic, aliphatic amino acids such as Leu and Nle, whereas the SHIP2 domain prefers a smaller residue such as Abu and Val. The most striking difference between the two SH2 domains, however, is their binding kinetics. For all six pY peptides tested in this work, which were derived from either library screening or known SHIP1/2 SH2 domain-binding sites in various receptor proteins, the SHIP1 SH2 domain showed

"normal" fast-on/fast-off kinetics, with half-lives of 1−3 s for the SH2−pY peptide complex. The SHIP2 SH2 domain, on the other hand, had 2 orders of magnitude slower association and dissociation rates against the six peptides and much longer half-lives (2−10 min) for the SH2-pY complex, as revealed by SPR analysis (Tables 3 and 4). More careful analysis suggested that the SHIP2 SH2 domain exists as a mixture of a small amount of exceptionally active P* form (~2.5%) and a large amount of inactive (or poorly active) P form (~97%). The observed "slow-binding" behavior is apparently a result of mass transport limitation. Presumably, the P form structure contains two *cis* peptidyl−prolyl imide bonds at Pro-88 and Pro-105, whereas the P* form has both bonds in the *trans* configuration. Pro-88 and Pro-105 are located in the EF and BG loops, respectively (*44*, *45*). These two loops form two walls of the binding pocket for the pY+3 residue. It is thus conceivable that a *cis*-prolyl residue(s) could disrupt this binding pocket and greatly reduce the binding affinity. Upon binding to a pY ligand, depletion of the free P* form would generate a driving force for converting more P form to the P* form. Apparently, the interconversion between P and P* is slow (if any) under the *in vitro* conditions employed for the SPR studies. *In vivo*, however, the interconversion may be catalyzed by a peptidyl−prolyl isomerase (e.g., cyclophilin), as has been shown for the Itk SH2 domain (*40*), and therefore the interaction between the SHIP2 SH2 domain and pY proteins may follow genuine slow-binding kinetics. Our preliminary studies showed that the interaction between full-length SHIP2 and several pY proteins *in vivo* indeed occurred more slowly than for SHIP1 (A.-S. Wavreille and S. Tridandapani, unpublished results).

Some of the functional differences between SHIP1 and SHIP2 can be attributed to their different expression patterns (*11*−*14*). This, however, cannot possibly explain their nonredundant roles in hematopoietic cells, where both enzymes are present. Other factors that may contribute to their different functions include the different substrate specificities of their phosphatase domains (*4*) and the presence of a SAM domain in SHIP2 (but not in SHIP1), which mediates protein−protein interaction via the formation of homo- and heterotypic oligomers (*46*). The present study reveals two additional factors that can potentially affect the biological functions of SHIP1 and SHIP2. First, the subtle specificity differences between the two SH2 domains may allow SHIP1 and SHIP2 to bind to different pY partner proteins or to bind to the same protein target with different affinities, both of which could result in different signaling outcomes. Second, the difference in binding kinetics may have important functional consequences. The fast association rates of SHIP1 SH2 domain suggests that, upon phosphorylation of the ITIM(s) or ITAM(s) of a receptor protein, SHIP1 would be immediately recruited to the receptor. At the same time, its fast dissociation would allow rapid exposure of the pY motif for dephosphorylation or binding to other proteins. In contrast, it would take a longer time for SHIP2 to bind to these receptors; once bound, however, SHIP2 would stay bound to the pY proteins for much longer periods of time, preventing their dephosphorylation or exchange with other protein partners. It is tempting to suggest that SHIP1 may function in signaling pathways that require fast- and short-lasting responses, whereas SHIP2 may function in processes that require prolonged signal duration. The requirement of *cis*−*trans* isomerization of a peptidyl−prolyl imide bond(s) may provide an interesting regulatory mechanism to modulate the interaction between SHIP2 and pY proteins. These possibilities are currently under investigation in our laboratory.

In conclusion, our study has shown that the two SH2 domains of SHIP1 and SHIP2 have similar binding specificities (though nonidentical) and the major difference is in their binding kinetics. Along with their differential tissue distribution, the differences in binding specificity and kinetics likely dictate the different biological functions of the two phosphatases. Our findings suggest that the kinetic difference may play a significant role in other protein−protein interactions and the isomerization of peptidyl−prolyl bonds may be a common mechanism for regulating the binding affinity and kinetics. Certainly, more attention should be paid to the kinetic properties of protein−protein and protein−ligand interactions.

ACKNOWLEDGMENT

We thank Dr. Susheela Tridandapani (The Ohio State University) for providing the SHIP2 gene and for valuable suggestions throughout the project.

REFERENCES

1. Berridge, M. J., and Irvine, R. F. (1989) Inositol phosphates and cell signaling. *Nature 341*, 197–205.
2. James, S. R., Downes, C. P., Gigg, R., Grove, S. J., Holmes, A. B., and Alessi, D. R. (1996) Specific binding of the Akt-1 protein kinase to phosphatidylinositol 3,4,5-trisphosphate without subsequent activation. *Biochem. J. 315*, 709–713.
3. Myers, M. P., Pass, I., Batty, I. H., Van der Kaay, J., Stolarov, J. P., Hemmings, B. A., Wigler, M. H., Downes, C. P., and Tonks, N. K. (1998) The lipid phosphatase activity of PTEN is critical for its tumor suppressor function. *Proc. Natl. Acad. Sci. U.S.A. 95*, 13513–13518.
4. Ooms, L. M., Horan, K. A., Rahman, P., Seaton, G., Gurung, R., Kethesparan, D. S., and Mitchell, C. A. (2009) The role of the inositol polyphosphate 5-phosphatases in cellular function and human diseases. *Biochem. J. 419*, 29–49.
5. Liu, Q., Oliveira-Dos-Santos, A. J., Mariathasan, S., Bouchard, D., Jones, J., Sarao, R., Kozieradzki, I., Ohashi, P. S., Penninger, J. M., and Dumont, D. J. (1998) The inositol polyphosphate 5-phosphatase ship is a crucial negative regulator of B cell antigen receptor signaling. *J. Exp. Med. 188*, 1333–1342.
6. Kalesnikoff, J., Lam, V., and Krystal, G. (2002) SHIP represses mast cell activation and reveals that IgE alone triggers signaling pathways which enhance normal mast cell survival. *Mol. Immunol. 38*, 1201–1206.
7. Liu, Q., Sasaki, T., Kozieradzki, I., Wakeham, A., Itie, A., Dumont, D. J., and Penninger, J. M. (1999) SHIP is a negative regulator of growth factor receptor-mediated PKB/Akt activation and myeloid cell survival. *Genes Dev. 13*, 786–791.
8. Ishihara, H., Sasaoka, T., Hori, H., Wada, T., Hirai, H., Haruta, T., Langlois, W. J., and Kobayashi, M. (1999) Molecular cloning of rat SH2-containing inositol phosphatase 2 (SHIP2) and its role in the regulation of insulin signaling. *Biochem. Biophys. Res. Commun. 260*, 265–272.
9. Clement, S., Krause, U., Desmedt, F., Tanti, J. F., Behrends, J., Pesesse, X., Sasaki, T., Penninger, J., Doherty, M., Malaisse, W., Dumont, J. E., Le Marchand-Brustel, Y., Erneux, C., Hue, L., and Schurmans, S. (2001) The lipid phosphatase SHIP2 controls insulin sensitivity. *Nature 409*, 92–97.
10. Ai, J., Maturu, A., Johnson, W., Wang, Y., Marsh, C. B., and Tridandapani, S. (2005) The inositol phosphatase SHIP-2 down regulates FcγR-mediated phagocytosis in murine macrophages independently of SHIP-1. *Blood 107*, 813–820.
11. Geier, S. J., Algate, P. A., Carlberg, K., Flowers, D., Friedman, C., Trask, B., and Rohrschneider, L. R. (1997) The human SHIP gene is differentially expressed in cell lineages of the bone marrow and blood. *Blood 89*, 1876–1885.
12. Liu, Q., Shalaby, F., Jones, J., Bouchard, D., and Dumont, D. J. (1998) The SH2-containing inositol polyphosphate 5-phosphatase, SHIP, is expressed during hematopoiesis and spermatogenesis. *Blood 91*, 2753–2759.
13. Pesesse, X., Deleu, S., De Smedt, F., Drayer, L., and Erneux, C. (1997) Identification of a second SH2-domain-conatining protein closely related to the phosphatidylinositol polyphosphate 5-phosphatase SHIP. *Biochem. Biophys. Res. Commun. 239*, 697–700.
14. Schurmans, S., Carrio, R., Behrends, J., Pouillon, V., Merino, J., and Clement, S. (1999) The mouse SHIP2 (Inppl1) gene: complementary

DNA, genomic structure, promoter analysis, and gene expression in the embryo and adult mouse. *Genomics 62*, 260–271.
15. Dyson, J. M., Munday, A. D., Kong, A. M., Huysmans, R. D., Matzaris, M., Layton, M. J., Nandurkar, H. H., Berndt, M. C., and Mitchell, C. A. (2003) SHIP-2 forms a tetrameric complex with filamin, actin, and GPIb-IX-V: localization of SHIP-2 to the activated platelet actin cytoskeleton. *Blood 102*, 940–948.
16. Giuriato, S., Pesesse, X., Bodin, S., Sasaki, T., Viala, C., Marion, E., Penninger, J., Schurmans, S., Erneux, C., and Payrastre, B. (2003) SH2-containing inositol 5-phosphatases 1 and 2 in blood platelets: their interactions and roles in the control of phosphatidylinositol 3,4,5-trisphosphate levels. *Biochem. J. 376*, 199–207.
17. Damen, J. E., Liu, L., Rosten, P., Humphries, R. K., Jefferson, A. B., Majerus, P. W., and Krystal, G. (1996) The 145-kDa protein induced to associate with Shc by multiple cytokines is an inositol tetraphosphate and phosphatidylinositol 3,4,5-trisphosphate 5-phosphatase. *Proc. Natl. Acad. Sci. U.S.A. 93*, 1689–1693.
18. Koncz, G., Toth, G. K., Bokonyi, G., Keri, G., Pecht, I., Medgyesi, D., Gergely, J., and Sarmay, G. (2001) Co-clustering of Fcγ and B cell receptors induces dephosphorylation of the Grb2-associated binder 1 docking protein. *Eur. J. Biochem. 268*, 3898–3906.
19. Liu, Y., Jenkins, B., Shin, J. L., and Rohrschneider, L. R. (2001) Scaffolding protein Gab2 mediates differentiation signaling downstream of Fms receptor tyrosine kinase. *Mol. Cell. Biol. 21*, 3047–3056.
20. van Dijk, T. B., Akker, E., Amelsvoort, M. P., Mano, H., Lowenberg, B., and von Lindern, M. (2000) Stem cell factor induces phosphatidylinositol 3′-kinase-dependent Lyn/Tec/Dok-1 complex formation in hematopoietic cells. *Blood 96*, 3406–3413.
21. Dunant, N. M., Wisniewski, D., Strife, A., Clarkson, B., and Resh, M. D. (2000) The phosphatidylinositol polyphosphate 5-phosphatase SHIP1 associates with the Dok1 phosphoprotein in Bcr-Abl transformed cells. *Cell. Signalling 12*, 317–326.
22. Lemay, S., Davidson, D., Latour, S., and Veillette, A. (2000) Dok-3, a novel adapter molecule involved in the negative regulation of immunoreceptor signaling. *Mol. Cell. Biol. 20*, 2743–2754.
23. Liu, L., Damen, J. E., Ware, M. D., and Krystal, G. (1997) Interleukin-3 induces the association of the inositol 5-phosphatase SHIP with SHP2. *J. Biol. Chem. 272*, 10998–11001.
24. Sattler, M., Salgia, R., Shrikhande, G., Verma, S., Choi, J. L., Rohrschneider, L. R., and Griffin, J. D. (1997) The phosphatidylinositol polyphosphate 5-phosphatase SHIP and the protein tyrosine phosphatase SHP-2 form a complex in hematopoietic cells which can be regulated by BCR/ABL and growth factors. *Oncogene 15*, 2379–2384.
25. Yogo, K., Mizutamari, M., Mishima, K., Takenouchi, H., Ishida-Kitagawa, N., Sasaki, T., and Takeya, T. (2006) Src homology 2 (SH2)-containing 5′-inositol phosphatase localizes to podosomes, and the SH2 domain is implicated in the attenuation of bone resorption in osteoclasts. *Endocrinology 147*, 3307–3317.
26. Roget, K., Malissen, M., Malbec, O., Malissen, B., and Daeron, M. (2008) Non-T cell activation linker promotes mast cell survival by dampening the recruitment of SHIP1 by linker for activation of T cells. *J. Immunol. 180*, 3689–3698.
27. Prasad, N., Topping, R. S., and Decker, S. J. (2001) SH2-containing inositol 5′-phosphatase SHIP2 associates with the p130^{Cas} adapter protein and regulates cellular adhesion and spreading. *Mol. Cell. Biol. 21*, 1416–1428.
28. Ono, M., Bolland, S., Tempst, P., and Ravetch, J. V. (1996) Role of the inositol phosphatase SHIP in negative regulation of the immune system by the receptor Fc(gamma)RIIB. *Nature 383*, 263–266.
29. Osborne, M. A., Zenner, G., Lubinus, M., Zhang, X., Songyang, Z., Cantley, L. C., Majerus, P., Burn, P., and Kochan, J. P. (1996) The inositol 5′-phosphatase SHIP binds to immunoreceptor signaling motifs and responds to high affinity IgE receptor aggregation. *J. Biol. Chem. 271*, 29271–29278.
30. Kimura, T., Sakamoto, H., Appella, E., and Siraganian, R. P. (1997) The negative signaling molecule SH2 domain-containing inositol-polyphosphate 5-phosphatase (SHIP) binds to the tyrosine-phosphorylated beta subunit of the high affinity IgE receptor. *J. Biol. Chem. 272*, 13991–13996.
31. Mason, J. M., Beattie, B. K., Liu, Q., Dumont, D. J., and Barber, D. L. (2000) The SH2 inositol 5-phosphatase Ship1 is recruited in an SH2-dependent manner to the erythropoietin receptor. *J. Biol. Chem. 275*, 4398–4406.
32. Muraille, E., Bruhns, P., Pesesse, X., Daeron, M., and Erneux, C. (2000) The SH2 domain containing inositol 5-phosphatase SHIP2 associates to the immunoreceptor tyrosine-based inhibition motif of FcγRIIB in B cells under negative signaling. *Immunol. Lett. 72*, 7–15.
33. Wang, Y. J., Keogh, R. J., Hunter, M. G., Mitchell, C. A., Frey, R. S., and Javaid, K.; et al. (2004) SHIP2 is recruited to the cell membrane upon macrophage colony-stimulating factor (M-CSF) stimulation and regulates M-CSF-induced signaling. *J. Immunol. 173*, 6820–6830.
34. Sweeney, M. C., Wavreille, A. S., Park, J., Butchar, J. P., Tridandapani, S., and Pei, D. (2005) Decoding protein-protein interactions through combinatorial chemistry: sequence specificity of SHP-1, SHP-2, and SHIP SH2 domains. *Biochemistry 44*, 14932–14947.
35. Sweeney, M. C., and Pei, D. (2003) An improved method for rapid sequencing of support-bound peptides by partial Edman degradation and mass spectrometry. *J. Comb. Chem. 5*, 218–222.
36. Thakkar, A., Wavreille, A. S., and Pei, D. (2006) Traceless capping agent for peptide sequencing by partial Edman degradation and mass spectrometry. *Anal. Chem. 78*, 5935–5939.
37. Bewarder, N., Weinrich, V., Budde, P., Hartmann, D., Flaswinkel, H., Reth, M., and Frey, J. R. (1996) In vivo and in vitro specificity of protein tyrosine kinases for immunoglobulin G receptor (FcγRII) phosphorylation. *Mol. Cell. Biol. 16*, 4735–4743.
38. Imhof, D., Wavreille, A.-S., May, A., Zacharias, M., Tridandapani, S., and Pei, D. (2006) Sequence specificity of SHP-1 and SHP-2 Src homology 2 domains: critical roles of residues beyond the pY+3 position. *J. Biol. Chem. 281*, 20271–20282.
39. Miller, M. L., Hanke, S., Hinsby, A. M., Friis, C., Brunak, S., Mann, M., and Blom, N. (2008) Motif decomposition of the phosphotyrosine proteome reveals a new N-terminal binding motif for SHIP2. *Mol. Cell. Proteomics 7*, 181–192.
40. de Mol, N. J., Catalina, M. I., Fischer, M. J. E., Broutin, I., Maier, C. S., and Heck, A. J. R. (2004) Changes in structural dynamics of the Grb2 adaptor protein upon binding of phosphotyrosine ligand to its SH2 domain. *Biochim. Biophys. Acta 1700*, 53–64.
41. Mallis, R. J., Brazin, K. N., Fulton, D. B., and Andreotti, A. H. (2002) Structural characterization of a proline-driven conformational switch within the Itk SH2 domain. *Nat. Struct. Biol. 9*, 900–905.
42. Schmid, F. X., and Baldwin, R. L. (1978) Acid catalysis of the formation of the slow-folding species of Rnase A: evidence that the reaction is proline isomerization. *Proc. Natl. Acad. Sci. U.S.A. 75*, 4764–4768.
43. Pesesse, X., Backers, K., Moreau, C., Zhang, J., Blero, D., Paternotte, N., and Erneux, C. (2006) SHIP1/2 interaction with tyrosine phosphorylated peptides mimicking an immunoreceptor signaling motif. *Adv. Enzymol. Regul. 46*, 142–153.
44. Waksman, G., Shoelson, S. E., Pant, N., Cowban, D., and Kuriyan, J. (1993) Binding of high affinity phosphotyrosyl peptide to the Src SH2 domain: crystal structures of the complexed and peptide-free forms. *Cell 72*, 779–790.
45. Eck, M. J., Shoelson, S. E., and Harrison, S. C. (1993) Recognition of a high-affinity phosphotyrosyl peptide by the Src homology-2 domain of p56^{lck}. *Nature 362*, 87–91.
46. Kim, C. A., and Bowie, J. U. (2003) SAM domains: uniform structure, diversity of function. *Trends Biochem. Sci. 28*, 625–628.
47. Larkin, M. A., Blackshields, G., Brown, N. P., Chenna, R., McGettigan, P. A., McWilliam, H., Valentin, F., Wallace, I. M., Wilm, A., Lopez, R., Thompson, J. D., Gibson, T. J., and Higgins, D. G. (2007) ClustalW and ClustalX version 2. *Bioinformatics 23*, 2947–2948.